Articles

Synthesis of Colloidal $CuGaSe_2$, $CuInSe_2$, and $Cu(InGa)Se_2$ Nanoparticles

Jiang Tang,[†] Sean Hinds,[‡] Shana O. Kelley,*[,§] and Edward H. Sargent*[,‡]

Department of Materials Science and Engineering, University of Toronto, 184 College Street, Room 140, Toronto, Ontario M5S 3E4, Canada, Department of Biochemistry and Faculty of Pharmacy, University of Toronto, Toronto, Ontario M5S 3M2, Canada, and Department of Electrical and Computer Engineering, University of Toronto, 10 King's College Road, Toronto, Ontario M5S 3G4, Canada

Received June 17, 2008. Revised Manuscript Received September 17, 2008

We synthesize $CuGaSe_2$, $CuInSe_2$, and $Cu(InGa)Se_2$ nanoparticles in oleylamine with narrow size distribution using commercial grade copper, indium, gallium salts, and Se powder. Tunable nanoparticle size and composition are achieved through manipulation of reaction temperature and precursor concentrations. Ternary and quaternary materials are engineered by the judicious matching of ligand−precursor reactivities.

Introduction

Colloidal nanoparticles, often derived from toxic heavy metals, are nevertheless versatile materials that yield low-cost, large-area, physically flexible photodetectors,[1a] photovoltaics,[1b,c] optical modulators,[1d] and optical sources.[1e,f] However, these materials often raise concern about their eventual environmental impact, especially if large-area deployment, such as in the case of solar cells, is sought. An attractive alternative is the synthesis of nontoxic $CuInS_2$, $CuInSe_2$, and $Cu(InGa)Se_2$ (CIGS). Polycrystalline CIGS films offer an alternative solar energy conversion material, providing both efficiencies up to 19.2%[2a] and excellent longevity.[2b]

The realization of third-generation solar cells having >30% AM1.5 power conversion efficiencies can be achieved by stacking semiconductors atop one another to form multijunction cells. A first cell absorbs higher-energy photons and provides a large open-circuit voltage; the next cells absorb lower-energy photons, and, series-connected, provide additive contributions to the open-circuit voltage. The layers of the optimal tandem AM1.5 (2-junction) cell have bandgaps at 1.3 um, near that of $CuInSe_2$, and 800 nm, near that of $CuGaSe_2$; they take the limiting efficiency up to 44% compared to the 32% limiting efficiency of an optimal single-junction device.[3]

Both the quantum size effect and control over stoichiometry enable synthetically controlled tuning in these materials systems. The following additionally important materials properties are required of the products of such a synthesis:

(1) purity of phase (to generate a single bandgap within each junction),

(2) colloidal stability and a lack of aggregation (to ensure practical processing), and

(3) excellent crystallinity (to provide sharp absorption onsets needed in optimized multijunction devices).

The synthesis of I−III−VI_2 ternary sulfide compounds has recently been extensively investigated but limited to $CuInS_2$ and $AgInS_2$.[4] In comparison, producing monodisperse I−III−VI_2 ternary and quaternary selenide-based chalcopyrite nanoparticles in solution remains challenging and/or underexplored. To the best of our knowledge, $CuGaSe_2$ nanoparticles synthesis in solution has not been reported previously. CIGS nanoparticles have been synthesized in methanol or pyridine at low temperature by a simple solvothermal route; however, these materials resulted in either large and uncontrolled aggregate formation[5a,b] or, unless annealed at elevated temperatures, generated amorphous materials.[5c] Synthesis of $CuInSe_2$ nanoparticles in solution has been reported elsewhere.[6]

* To whom correspondence should be addressed. E-mail: shana.kelley@utoronto.ca (S.O.K.); ted.sargent@utoronto.ca (E.H.S.).
[†] Department of Materials Science and Engineering, University of Toronto.
[‡] Department of Electrical and Computer Engineering, University of Toronto.
[§] Department of Biochemistry and Faculty of Pharmacy, University of Toronto.

(1) (a) Konstantatos, G.; Howard, I.; Fischer, A.; Hoogland, S.; Clifford, J.; Klem, E.; Levina, L.; Sargent, E. H. *Nature* **2006**, *442*, 180–183. (b) Gur, I.; Fromer, N. A.; Geier, M. L.; Alivisatos, A. P. *Science* **2005**, *310*, 462–464. (c) Johnston, K. W.; Pattantyus-Abraham, A. G.; Clifford, J. P.; Myrskog, S. H.; MacNeil, D. D.; Levina, L.; Sargent, E. H. *Appl. Phys. Lett.* **2008**, *92*, 151115. (d) Hoogland, S.; Sukhovatkin, V.; Shukla, H.; Clifford, J.; Levina, L.; Sargent, E. H. *Opt. Express* **2008**, *16*, 6683–6691. (e) Tessler, N.; Medvedev, V.; Kazes, M.; Kan, S.; Banin, U. *Science* **2002**, *295*, 1506–1508. (f) Konstantatos, G.; Huang, C.; Levina, L.; Lu, Z.; Sargent, E. H. *Adv. Funct. Mater.* **2005**, *00*, 1–6.

10.1021/cm801655w CCC: $40.75
Published on Web 10/28/2008

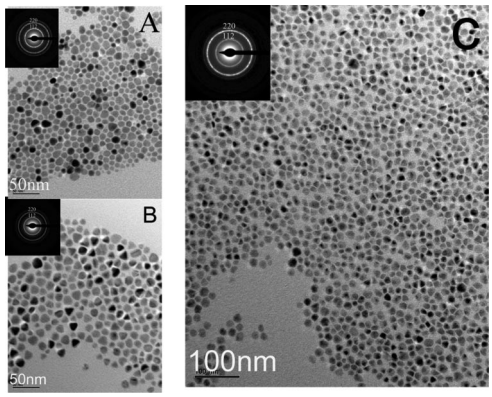

Figure 1. TEM images of chalcopyrite nanoparticles synthesized herein and their corresponding SAED pattern: (A) $CuGaSe_2$, (B) $CuInSe_2$, and (C) CIGS.

Here we report the synthesis of $CuGaSe_2$, $CuInSe_2$, and CIGS nanoparticles in oleyamine using hot injection methods. The principles that guided our approach were as follows:

Rapid formation of chalcopyrite compounds is observed in mixtures of appropriate precursors with liquid Se;[7]

Cu, In, and Ga salts as well as selenium powders dissolve in oleyamine at elevated temperatures and enable chalcopyrite nanoparticle formation;[8]

The reactivities of precursors must favor ternary and quaternary compound formation and avoid binary compounds in a successful synthesis.[9]

On the basis of the the preceding strategy, we synthesize nearly monodisperse $CuGaSe_2$, $CuInSe_2$, and CIGS nanoparticles using only commercial salts, selenium powder, and oleylamine. Herein we characterize their morphology, absorption spectra, and photoresponse. Our synthesis marks an advance for chalcopyryte nanomaterial solar cells and offers a possible template for the synthesis of other ternary and quaternary nanomaterials.

(2) (a) Ramanathan, K.; Contreras, M. A.; Perkins, C. L.; Asher, S.; Hasoon, F. S.; Keane, J.; Young, D.; Romero, M.; Metzger, W.; Noufi, R.; Ward, J.; Duda, A. *Prog. Photovolt: Res. Appl.* **2003**, *11*, 225–230. (b) Guillemoles, J. F.; Kronik, L.; Rau, D. C. U.; Jasenek, A.; Schock, H. W. *J. Phys. Chem. B* **2000**, *104*, 4849–4862.

(3) Martí, A.; Araújo, G. L. *Sol. Energy Mater. Sol. Cells* **1996**, *43*, 203–222.

(4) (a) Wang, D. S.; Zheng, W.; Hao, C. H.; Peng, Q.; Li, Y. D. *Chem. Commum.* **2008**, 2556–2558. (b) Pan, D.; An, L.; Sun, Z.; Hou, W.; Yang, Y.; Yang, Z.; Liu, Y. *J. Am. Chem. Soc.* **2008**, *130*, 5620–5621. (c) Tian, L.; Elim, H. I.; Ji, W.; Vittal, J. J. *Chem. Commun.* **2006**, 4276–4278.

(5) (a) Ahn, S.; Kimb, K. H.; Yoon, K.-H. *Thin Solid Films* **2007**, *515*, 4036–4040. (b) Chuna, Y. G.; Kimb, K. H.; Yoon, K. H. *Thin Solid Films* **2005**, *480*, 46–49. (c) Schulz, D. L.; Curtis, C. J.; Flitton, R. A.; Wiesner, H.; Keane, J.; Matson, R. J.; Jones, K. M.; Parilla, P. A.; Noufi, R.; Ginley, D. S. *J. Electron. Mater.* **1998**, *27*, 433–437.

(6) (a) Azad, M. M.; O'Brien, P.; Revaprasadu, N. *Adv. Mater.* **1999**, *11*, 1441–1444. (b) Yang, Y. H.; Chen, Y. T. *J. Phys. Chem. B* **2006**, *110*, 17370–17374. (c) Zhong, H.; Li, Y.; Ye, M.; Zhu, Z.; Zhou, Y.; Yang, C.; Li, Y. F. *Nanotechnology* **2007**, *18*, 025602–025607. (d) Peng, H. L.; Schoen, D. T.; Meister, S.; Zhang, X. F.; Cui, Y. *J. Am. Chem. Soc.* **2007**, *129*, 34–35.

(7) Hergerta, F.; Josta, S.; Hocka, R.; Purwins, M. *J. Solid State Chem.* **2006**, *179*, 2394–2415.

(8) (a) Park, K. H.; Jang, K.; Kim, S. Y.; Kim, H. J.; Son, S. U. *J. Am. Chem. Soc.* **2006**, *128*, 14780–14781. (b) Wang, Y. H. A.; Bao, N.; Shen, L. M.; Padhan, P.; Gupta, A. *J. Am. Chem. Soc.* **2007**, *129*, 12408–12409.

(9) Matsushita, H.; Takizawa, T. *J. Cryst. Growth* **1997**, *179*, 503–509.

Experimental Section

Chemicals. Copper(I) acetate (CuAc), copper(II) acetylacetonate ($Cu(acac)_2$), indium(III) chloride ($InCl_3$), indium(III) acetylacetonate ($In(acac)_3$), gallium(III) acetylacetonate ($Ga(acac)_3$), selenium powder (Se), and technical grade oleylamine (70%) were all purchased from Sigma-Aldrich. Oleylamine, used throughout, was pumped under a vacuum at 80 °C for 12 h before use. Our experience indicated that golden-yellow oleylamine with some white flocculates produced better results. All other chemicals were used as received.

Preparation of $CuGaSe_2$, $CuInSe_2$, and CIGS Nanoparticles. All syntheses were carried out using a Schlenk line. A round two-necked flask was placed in a heating mantle; one neck was connected to a condenser and the other was sealed by a septum. A thermocouple was inserted through the septum and into the mixture to provide accurate temperature control for the reaction. A typical procedure of $CuGaSe_2$ synthesis follows 0.2 mmol of $Cu(acac)_2$, 0.2 mmol of $Ga(acac)_3$, and 5 mL of oleylamine mixed at room temperature and then kept at 80 °C under vacuum for 1 h; afterward, we observe the precursors have completely dissolved. This solution was marked solution A. An 8 mL portion of oleylamine and 0.4 mmol of Se powder were deposited in a separate flask, vacuum pumped at 120 °C for 0.5 h, and then put under a N_2 atmosphere for the remainder of the synthetic reaction. This solution, labeled solution B, was then heated to 250 °C over a 10 min period and kept at that temperature. Over the course of an hour, the solution gradually changed from colorless, to orange, and to brownish red because of the dissolution of Se powder in oleylamine. Once the Se, from solution B, was completely dissolved, 5 mL of solution A was injected into it under vigorous stirring. The solution turned immediately to deep black; the heating mantle was then turned off to provide slow cooling of the reaction vessel. After 15 min, the temperature decreased to 100 °C, at which point the solution was heated again to 250 °C and incubated for one additional hour. Subsequently, the reaction mantle was removed and the reaction vessel was allowed to cool to room temperature. The solution was then transferred to test tubes and 5 mL of anhydrous methanol was added to the mixture; this mixture was then centrifugated at 3000 rpm for 1 min. The clear supernatant was discarded and its precipitate was redispersed in 10 mL anhydrous toluene. A 5 mL portion of methanol was added to the solution and the nanoparticles were again isolated by centrifugation. After the supernatant was again decanted, the precipitates were redispersed in 8 mL of anhydrous toluene; the suspension was centrifugated at 3000 rpm for 1 min, yielding little sediment and a brown-colored supernatant that was kept as the final product.

In the synthesis of other chalcopyrite nanoparticles, the above procedure is followed exactly with the exception of 0.2 mmol $InCl_3$, yielding $CuInSe_2$ nanomaterials, and 0.1 mmol of $In(acac)_3$ with 0.1 mmol of $Ga(acac)_3$, yielding $Cu(InGa)Se_2$ nanomaterials, respectively.

Structural, Optical, and Electrical Characterization of Chalcopyrite Nanoparticles. Transmission electron microscopy (TEM) and selected area electron diffraction (SAED) were used to characterize the nanomaterials. An EOL-2010-FEG microscope equipped with a tungsten filament and operated under accelerating voltage of 200 kV was employed. Powder X-ray diffraction (XRD) measurements were carried out in a Siemens diffractometer with Cu Kα radiation ($\lambda = 1.54178$Å). Vis−NIR absorption spectra of the nanomaterials in toluene were recorded at room temperature using a Cary 500 UV/vis/near-IR spectrophotometer. Fourier Transform Infrared Spectroscopy (FTIR) was carried out using a Bruker Tensor 27 Infrared Spectrometer. Samples were prepared by drop-casting CIGS nanoparticles onto KBr substrates, after which

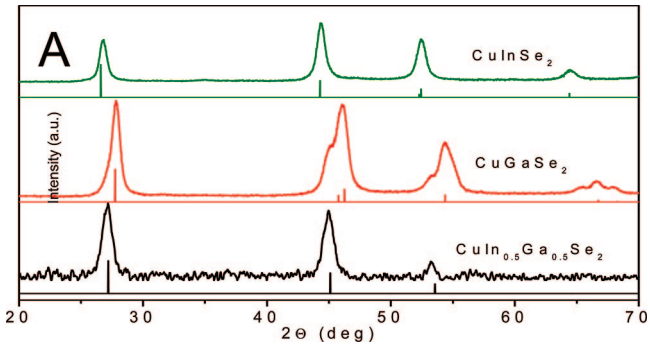

Figure 2. Powder XRD patterns of $CuGaSe_2$, $CuInSe_2$ and CIGS nanoparticles. The vertical lines below indicate the corresponding reflection peaks for bulk $CuIn_{0.5}Ga_{0.5}Se_2$ (JCPDS 40−1488), $CuGaSe_2$ (JCPDS 79−1809), and $CuInSe_2$ (JCPDS 40−1487).

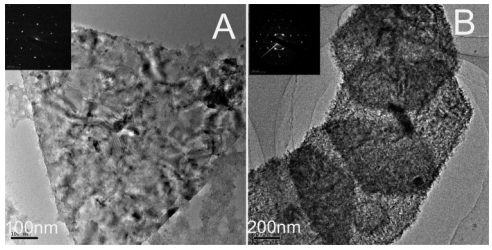

Figure 3. TEM images and corresponding SAED of (A) $CuGaSe_2$ and (B) $CuInSe_2$ hexagonal microplates obtained in oleylamine and oleic acid mixture.

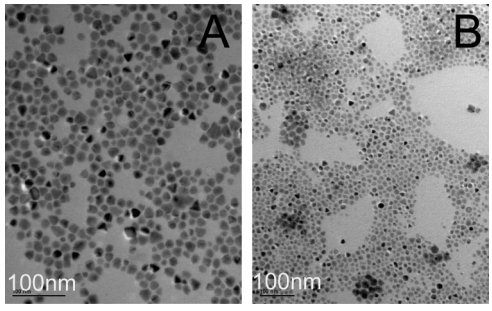

Figure 4. TEM images of CIGS nanoparticles synthesized by injecting $Cu(acac)_2$, $In(acac)_3$, and $Ga(acac)_3$ oleylamine solution into Se/oleylamine at different injection temperatures: (A) 270 and (B) 220 °C.

the samples were dried in air. ICP measurements were performed using a Perkin-Elmer Model Optima 3000DV ICP AEOS. Samples prepared for electrical characterization were made by drop-casting 20 μL of concentrated nanoparticle solution in toluene onto a quartz glass with interdigitated gold electrodes (IDE). The gap between gold electrodes is 2.5 μm and their length is 3 mm. The thickness of film was measured to be approximately 1 μm using a surface profiler (Veeco Dektak3). Current−voltage characteristics were acquired using an Agilent 4155C semiconductor parameter analyzer, its scanning voltage tuned from 0 to 10 V.

Results and Discussion

The size and morphology of as-synthesized chalcopyrite nanomaterials were characterized by TEM. Typical results are shown in Figure 1. Figure 1A shows TEM images of platelike $CuGaSe_2$ nanoparticles with an average size of 11 nm. $CuInSe_2$ nanoparticles (Figure 1B) were a mixture of triangular, hexagonal, and round platelike nanoparticles with an average size of 16 nm. CIGS nanoparticles had an average diameter of 15 nm, most of which had triangular morphology. All these syntheses show a narrow size distribution, shown in the histograms of their size distributions (see the Supporting Information, Figure S1). To the best of our knowledge, this represents the first report of narrowly size-distributed solution-synthesized $CuGaSe_2$ and CIGS nanoparticles. The median spacing between any two nanoparticles in all samples was approximately 2.4 nm, twice the length of oleylamine, indicating they were well passivated and protected by it. This assumption is confirmed by FTIR observation of feature peaks of oleylamine in as-synthesized nanoparticles, as shown in the Supporting Information, Figure S2. Oleylamine impedes carrier transport in nanoparticle films; removal of oleylamine using thermal annealing and chemical treatment such as hydrazine or ethanethiol have previously been shown[10] to lead to improved electrical and optoelectronic properties. The crystalline nature of nanoparticles is supported by their SAED patterns, included as figure insets.

Table 1. Composition of CIGS Nanoparticles Calculated from Inductively Coupled Plasma Atomic Emission Spectrometry (ICP)

precursor atomic ratio Cu:Ga:In:Se	Cu at %	Ga at %	In at %	Se at %	calcd formula
4:2:2:8	27.7	10.1	12.1	50.1	$CuGa_{0.36}$ $In_{0.44}Se_{1.81}$
4:3:1:8	28.4	13.4	8.5	49.7	$CuGa_{0.47}In_{0.30}Se_{1.75}$
3:2:2:8	23.0	9.5	17.9	49.6	$CuGa_{0.41}$ $In_{0.78}Se_{2.16}$

Figure 2 shows the XRD patterns of as-synthesized $CuGaSe_2$, $CuInSe_2$, and CIGS nanoparticles. All diffraction peaks follow their standard bulk crystal structure patterns for $CuGaSe_2$ (JCPDS 79−1809), $CuInSe_2$ (JCPDS 40−1487), and $Cu(In_{0.5}Ga_{0.5})Se_2$ (JCPDS 40−1488), respectively. For each type of synthesis we observe these nanomaterials possess a low-temperature tetragonal phase composition. Their diffraction peaks suggest side products, or impurities, were not significantly present in the samples. Nanoparticle sizes calculated from the Scherrer equation were 10.8 nm, 16.5 and 15.2 nm for $CuGaSe_2$, $CuInSe_2$, and CIGS nanoparticles, respectively, well agreed with the above-described TEM observations.

We found that organometallic hot injection, as well as a specific choice of ligands and precursors, as described above, was crucial to this synthetic method. Syntheses that employed ligands such as trioctylphosphine, trioctylphosphine oxide,

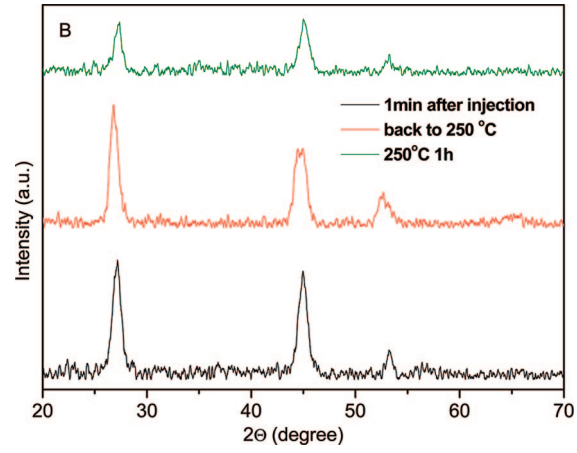

Figure 5. XRD patterns of CIGS nanoparticles arrested for different reaction durations.

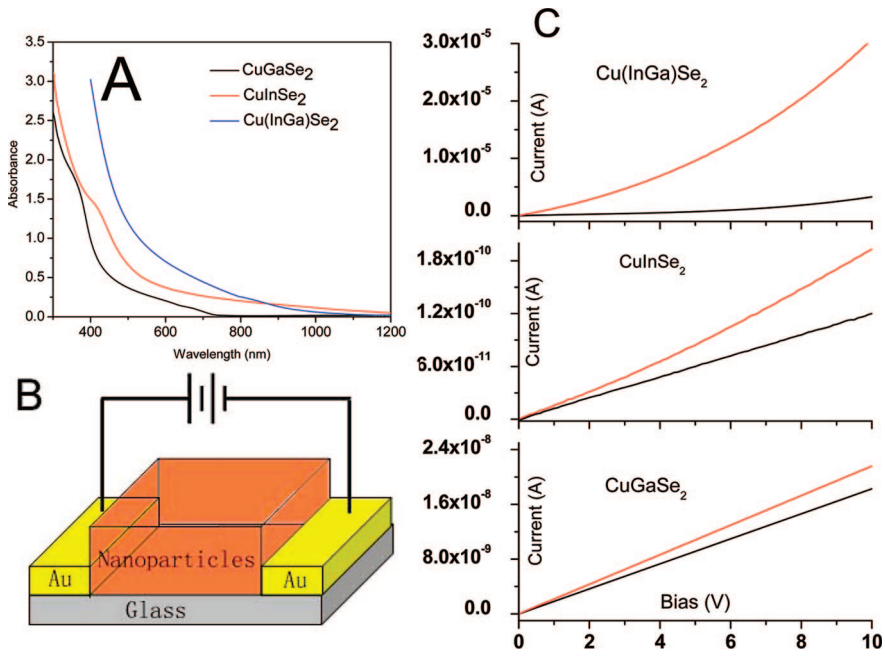

Figure 6. (A) Ensemble of UV−vis−NIR absorption spectrum of $CuGaSe_2$, $CuInSe_2$, and $Cu(InGa)Se_2$ nanoparticles in toluene. (B) Schematics of device configuration for photoresponse measurement. (C) $I-V$ curves of drop-casting films built from $CuGaSe_2$, $CuInSe_2$, and $Cu(InGa)Se_2$ nanoparticles: in the dark (black) and under lamp illumination (red).

dodecanethiol, oleic acid, stearic acid, and combinations thereof, all failed. Syntheses yielding single-crystalline $CuGaSe_2$ and $CuInSe_2$ trigonal and/or hexagonal microplates were obtained through the use of a mixture of oleylamine and oleic acid. Separated diffraction points with hexagonal symmetry were observed in SAED pattern, as included in Figure 3A and B, suggesting their single-crystalline nature. When all precursors were simply mixed and heated up to 250 °C in oleylamine, both $CuGaSe_2$ and $CuInSe_2$ nanoparticles with a very wide size distribution, one that included large aggregates, were obtained (see the Supporting Information, Figure S3). We attribute this to the simultaneous dissolution of Se powder in oleylamine combined with nucleation and growth of nanoparticles during this process, conditions that fail to achieve the slow size-focusing growth after a rapid nucleation burst needed for monodispersed nanoparticle synthesis. In addition, we noted that a poor choice of precursors always led to poor products in the form of a secondary phase and/or polydispersity (see the Supporting Information, Figure S4). In summary, our general strategy relied on the careful choice of precursor and ligand combinations in synthesizing these ternary and quaternary nanomaterials.[11] Without careful reactivity-matching, a plurality of phases and/or broad size distribution of products were obtained.

We found that the size as well as the composition of CIGS nanoparticles was tunable by employing the above synthesis. When the injection temperature varied from 220 to 270 °C and all other parameters were kept constant, the average size of $Cu(InGa)Se_2$ nanoparticles tuned from 12 to 18 nm, as shown in Figure 4. Generally, higher injection temperature favors the growth of larger nanoparticles. When the precursor molar ratio of $Cu(acac)_2$:$Ga(acac)_3$:$In(acac)_3$:Se changed from 4:2:2:8, to 4:3:1:8, and to 3:2:2:8 the composition of as-synthesized nanoparticles, determined by ICP was $CuGa_{0.38}In_{0.41}Se_{1.87}$, $CuGa_{0.47}In_{0.30}Se_{1.75}$, and $CuGa_{0.41}In_{0.83}Se_{1.98}$, respectively (see the Supporting Information, Figure S5, for TEM and XRD patterns). The observed deviation of product stoichiometry from precursor ratios is attributed to modestly different reactivities of the metal precursors; Table 1 summarizes the precursor applied and the final products composition. Our experience showed $In(acac)_3$ is more reactive than $Ga(acac)_3$ in our system and some intermediates and/or precursors present in the final products judged from ICP-AES results. Precise composition control of such ternary and quaternary nanomaterials remains challenging and further exploration is recommended.

To study the mechanism of the reaction, we took a 1 mL aliquot of the reaction solution 1 min after the injection of solution A into solution B and characterized it by XRD. From the XRD patterns, shown in Figure 5, we observe that products show exclusively $Cu(In_{0.5}Ga_{0.5})Se_2$ diffraction peaks, implying chalcopyrite nanoparticles formed rapidly upon injection. In our synthesis, Cu^{2+} and Se were reduced to Cu^+ and Se^{2-} in $Cu(InGa)Se_2$ nanoparticles and oleylamine was believed to be oxidized. In fact, oleylamine has been proposed to reduce sulfur and selenium in the synthesis of sulfide[12a] and selenide[12b] nanoparticles; and Malakooti et al. proposed that the amine group is oxidized into a nitroso group.[12c] Clearly, the detailed reaction pathway requires further elucidation.

To evaluate the application of this synthetic method toward solution-processed solar cells, we studied their optoelectronic

(10) (a) Talapin, D. V.; Murray, C. B. *Science* **2005**, *310*, 86–89. (b) Kovalenko, M. V.; Heiss, W.; Shevchenko, E. V.; Lee, J. S.; Schwinghammer, H.; Alivisatos, A. P.; Talapin, D. V. *J. Am. Chem. Soc.* **2007**, *129*, 11354–11355. (c) Luther, J. M.; Law, M.; Song, Q.; Perkins, C. L.; Beard, M. C.; Nozik, A. J. *ACS Nano* **2008**, *2*, 271–280.

(11) (a) Bao, N.; Shen, L.; Wang, Y.; Padhan, P.; Gupta, A. *J. Am. Chem. Soc.* **2007**, *129*, 12374–12375. (b) Du, W. M.; Qian, X. F.; Yin, J.; Gong, Q. *Eur. Chem. J.* **2007**, *13*, 8840–8846.

properties. The absorption spectra of as-synthesized $CuGaSe_2$, $CuInSe_2$, and $Cu(InGa)Se_2$ nanoparticles in toluene are presented in Figure 6A. The absorption onset of $CuGaSe_2$ and $CuInSe_2$ at 729 nm (1.70 eV) and 1200 nm (1.03 eV) is consistent with their bulk band gap energies of 1.68 and 1.01 eV, respectively. $Cu(InGa)Se_2$ nanoparticles showed strong absorption from 1000 nm, corresponding to band gap of 1.2 eV, the optimal value for single-junction solar cells. To study the materials' optoelectronic properties, we first produced smooth, $\sim$1 μm thick films by drop-casting concentrated toluene solutions of $CuGaSe_2$, $CuInSe_2$, and $CuInGaSe_2$ nanoparticles onto interdigitated electrode (IDE) glass test chips. The $I-V$ curves, shown in Figure 6C, for $Cu(InGa)Se_2$, $CuGaSe_2$, and $CuInSe_2$ nanoparticles all show photoresponse. The current of CIGS film at 10 V changed from 3.28×10^{-6} A in the dark to 3.07×10^{-5} A when the lamp light was on, a 10-fold increase.

Conclusions

In this study, we have demonstrated a synthesis of $CuGaSe_2$, $CuInSe_2$, and CIGS nanoparticles by careful adjustment of precursors and ligands. Photoresponse from drop-cast film of these nanoparticles was also observed. Our preliminary experiments indicate this approach is also applicable to $CuInS_2$ and $CuGaS_2$ synthesis using sulfur powder instead of selenium powder.[13] Tuning the size and composition of the materials combined with their low-cost precursors and initial photoresponse suggest promise in optical and electronic applications.

Acknowledgment. We thank Chad J. Dooley at the Department of Chemistry, Boston College, and Dr. Larissa Levina at the Department of Electrical and Computer Engineering, University of Toronto, for their help during the course of this study.

Supporting Information Available: FTIR, TGA, statistic histogram of size distribution, XRD, TEM, and SAED (PDF). This material is available free of charge via the Internet at http://pubs.acs.org.

CM801655W

(12) (a) Joo, J.; Na, H. B.; Yu, T.; Yu, J. H.; Kim, Y. W.; Wu, F. X.; Zhang, J. Z.; Hyeon, T. *J. Am. Chem. Soc.* **2003**, *125*, 11100. (b) Park, K. H.; Jang, K. J.; Kim, S. Y.; Kim, H. J.; Son, S. K. *J. Am. Chem. Soc.* **2006**, *128*, 14780. (c) Malakooti, R.; Cademartiri, L.; Akcakir, Y.; Petrov, S.; Migliori, A.; Ozin, G. A. *Adv. Mater.* **2006**, *18*, 2189.
(13) Please see Figure S6 in the Supporting Information.